ChemPubSoc Europe
DOI: 10.1002/celc.201500022
CHEMELECTROCHEM Articles

Promotional Effect of Ag on the Catalytic Activity of Au for Glycerol Electrooxidation in Alkaline Medium

Amanda C. Garcia,[b] Julia Caliman,[a] Eduardo B. Ferreira,[b] Germano Tremiliosi-Filho,[b] and José J. Linares*[a]

The potential of silver as an auxiliary metal for gold in the electrochemical oxidation of glycerol in alkaline medium is studied. Three bimetallic materials (Au_3Ag/C, AuAg/C, and $AuAg_3/C$) and the corresponding monometallic reference materials (Au/C and Ag/C) are prepared by chemical reduction of their precursors with glycerol. Half-cell measurements evidence the beneficial effect of Ag on the electrocatalytic activity of Au for glycerol oxidation owing to decreased onset potential and higher current density in chronoamperometry, with an optimum formulation of AuAg/C. These results are confirmed by the single-cell performance of AuAg/C, which, despite having half the Au loading, has a higher open-circuit voltage than Au/C and a similar maximum power density. The results are correlated with the structural and electronic features of these materials, which are widely discussed in other works.

1. Introduction

In the search for a more diverse and sustainable mix of power sources as an alternative to fossil fuels, renewable energy is gaining relevance.[1] Biofuels such as bioethanol and biodiesel belong to this new generation of energy sources.[2] In particular, the biodiesel industry experienced exponential growth in the last two decades and is expected to continue expanding owing to the worldwide government policies on investing in biofuels.[1] Biodiesel is produced by the transesterification reaction between a vegetable oil or animal fat and an alcohol, usually methanol. The coproduct of this reaction is glycerol (glycerin or propan-1,2,3-triol), which was traditionally used by the pharmaceutical and cosmetic industries, among others. However, the present production rate has already surpassed the capacity of these classical industries, and therefore new strategies to valorize glycerol are necessary.[3–8]

One of the proposed alternative uses for glycerol is as a fuel in a direct glycerol fuel cell (DGFC).[9–22] Complete oxidation of the glycerol molecule produces 14 electrons, although its incomplete oxidation to mesoxalic acid can produce 10 electrons and 8 electrons if tartronic acid is the main product (most typical C_3 products).[16] Furthermore, DGFCs can compete well with the two most classical fuels for liquid fuel cells, methanol and ethanol, in terms of energy density (5.0 versus 6.1 and 8.1 kWh kg^{-1} for methanol and ethanol, respectively).[13] In this way, it is possible to obtain energy from glycerol electrooxidation in addition to added-value oxidation products, such as tartronic, mesoxalic, and β-hydroxypyruvic acids, as well as dihydroxyacetone, as widely demonstrated by recent papers.[15,16,23–26] In the studies by Xin et al.,[23] Zhang et al.,[17,24–26] Padayachee et al.,[27] and Yongprapat et al.,[19,20] the potential of Au/C as an anode material for DGFCs in alkaline medium was demonstrated. They also showed the possibility of tuning both the electrochemical performance and the product distribution by modifying the size of gold nanoparticles and the cell/anode potential. However, one of the shortcomings of Au/C compared to the other two classical monometallic catalysts, Pd/C and Pt/C, is the higher onset potential for glycerol electrooxidation. The reason for this is the higher potential required for the appearance of oxygenated species on the gold surface.[28] In this regard, an important finding was recently presented by Padayachee et al.,[27] who showed that lower onset potential can be achieved by small gold nanoparticles having predominantly Au(110) facets. Another classical approach for decreasing the onset potential of any alcohol electrooxidation process is the addition of less noble metal to exploit the well-known bifunctional mechanism.[29] Silver has already been demonstrated to be a promising auxiliary metal for glycerol electrooxidation in alkaline medium,[30–34] because it increases the maximum current density and reduces the onset potential for alcohol oxidation. Silver may supply oxygenated species to the gold surface and, more importantly, in an alkaline environment, it can modify the electronic environment of gold.[31]

Tremiliosi et al. recently developed a simple and green method for the preparation of Au, Ag, and AuAg catalysts with glycerol as reducing agent.[32–35] They discussed in detail the structural and electronic features of the materials, especially

[a] J. Caliman, Dr. J. J. Linares
Instituto de Química
Universidade de Brasília
Campus Universitário Darcy Ribeiro
CP 4478 CEP 70910-900, Brasília, DF (Brazil)
E-mail: joselinares@unb.br

[b] Dr. A. C. Garcia, E. B. Ferreira, Prof. G. Tremiliosi-Filho
Instituto de Química de São Carlos
Universidade de São Paulo
Av. Trabalhador Sãocarlense
400 CP 780 CEP 13560-970
São Carlos, SP (Brazil)

the bimetallic AuAg materials, through a combination of experimental techniques and molecular dynamic simulations, which evidenced the formation of a core–shell-like structure with a gold core and an Ag-enriched AuAg alloy shell (the higher the Au content, the higher the degree of alloying).[34] Garcia et al.[32] also reported that Ag decreases the occupancy of the Au 5d band, with a consequent electronic effect that affects the adsorption strength of eventual adsorbates. This is also expected to affect the electrochemical response of the bimetallic AuAg towards glycerol electrooxidation, as preliminarily evidenced in those works. Complementary to the previous works, the scope of this study was a more systematic analysis of the electrochemical response of these materials. In this regard, we analyzed the effect of Ag on the electrochemical activity of Au for glycerol electrooxidation. Cyclic voltammograms (CVs) and chronoamperometric curves were recorded in a three-electrode cell and compared to those of monometallic reference materials. Subsequently, the best bimetallic material and Au/C were used to prepare fuel-cell electrodes. KOH-doped polybenzimidazole (PBI)-based alkaline membrane electrode assemblies (MEAs) were manufactured and tested at different temperatures, and the corresponding polarization curves were obtained. To better comprehend the electrochemical results, they were correlated to the structural characteristics of the catalysts.

2. Results and Discussion

Figure 1 shows the CVs of the different catalysts in the blank 1 mol L^{-1} KOH solution, from which enlightening information

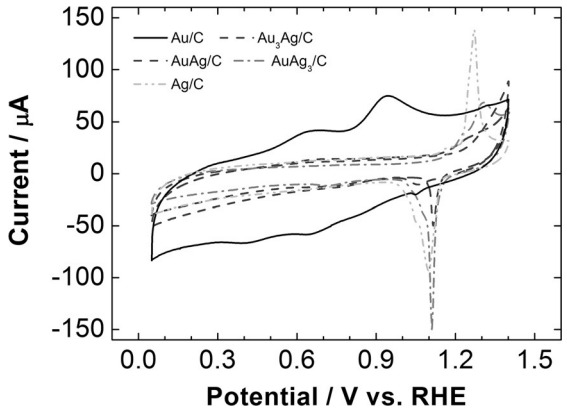

Figure 1. CVs of the different catalysts at 25 °C and a scan rate of 10 mV s^{-1} in 1 mol L^{-1} KOH.

can be extracted, especially for the bimetallic materials. Ag/C shows a marked redox pair associated with Ag/Ag_2O species, the reduction peak of which is at approximately 1.1 V versus RHE.[36,37] These peaks remains intense for $AuAg_3$/C and are diminished for AuAg/C, whereas they are only weakly perceptible for Au_3Ag/C, the profile of which in this region more resembles that of Au/C, with a very weak peak for the reduction of gold oxide at approximately 1.05 V versus RHE. Such tiny peaks can be attributed to the low metal content in the catalysts (ca. 10% on the carbon support), as recently shown in the literature.[38,39] Since cyclic voltammetry can be considered to be a "surface radiography" technique, the observed profiles are a sign of decreasing Ag content in the surface of the bimetallic materials with decreasing silver content. It is even conceivable that Au_3Ag/C could have an almost exclusively Au surface. However, Gomes et al.[34] already demonstrated that even the Au-rich Au_3Ag/C has an Ag-rich surface shell. Such a contradiction can be explained in terms of the observation of Sobyanin et al.,[40] who reported a decrease in the ability of Ag to adsorb oxygenated species with decreasing Ag content in Au/Ag materials. On the basis of the Au core/Ag-rich shell structure, the higher the Au content, the closer the core comes to the particle surface. This may explain the effect observed by Sobyanin et al. and, with the consequent disappearance of the reduction peaks for silver oxide, supports the electronic effects observed by Garcia et al.[32] and further corroborates the layered structure proposed in previous works.[34]

The glycerol electrooxidation profiles of the different materials are depicted in Figure 2. Due to the uncertainties in esti-

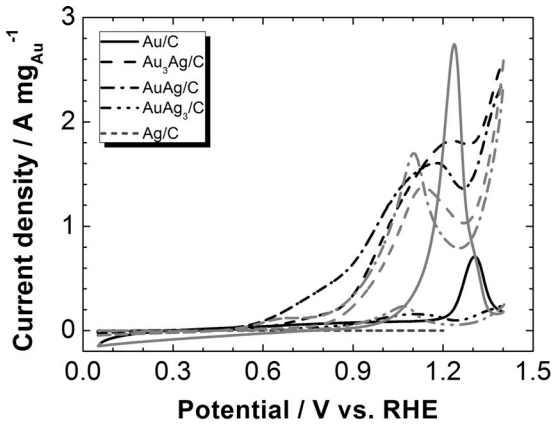

Figure 2. CVs of the different catalysts at 25 °C and a scan rate of 10 mV s^{-1} in 1 mol L^{-1} KOH and 1 mol L^{-1} glycerol (black lines correspond to the forward scan).

mating the electrochemically active area from the metal-oxide reduction peaks, all of the electrochemical results were mass-normalized with respect to the gold loading, on the basis of the inactivity shown by the Ag/C material. Table 1 lists some key data from the voltammograms, except for that of the inac-

Table 1. Onset potential for glycerol electrooxidation, forward (i_f) and backward (i_b) maximum current density, and i_f/i_b ratios (values for Ag/C are not presented due to zero activity for glycerol electrooxidation).

Catalyst	Onset potential [V]	i_f [A mg_{Ag}^{-1}]	i_b [A mg_{Ag}^{-1}]	i_f/i_b
Au/C	1.09	0.705	2.74	0.257
Au_3Ag/C	0.610	1.81	1.35	1.34
AuAg/C	0.511	1.60	1.68	0.941
$AuAg_3$/C	0.625	0.144	0.222	0.649

tive Ag/C, such as the onset potential (forward scan), the maximum current density for the forward and backward scans (i_f and i_b), and the i_f/i_b ratios. In the positive scan, the onset potential of Au/C is much higher than those of the bimetallic materials. This is already a first indication of the positive effect of silver on gold, leading to activation of glycerol electrooxidation. Of the bimetallic materials, AuAg/C has the lowest onset potential, which indicates a synergic interaction between Ag and Au that activates the gold surface at lower potential. Au/C shows an absolute maximum current density of 0.705 A mg_{Ag}^{-1}, whereas the bimetallic materials interestingly show relative maxima. The corresponding values of the forward first maxima for Au_3Ag/C and AuAg/C are larger than that of Au/C. However, that of $AuAg_3/C$ is significantly smaller, most likely due to a large fraction of silver in the particle surface. Hence, Au_3Ag/C and AuAg/C appear to be the most suitable materials for glycerol electrooxidation.

Interestingly, the CVs are different to those presented in refs. [32, 33]. The reason for this is the distinct reaction medium used in this study. In this case, a higher electrolyte concentration (1 mol L^{-1}) and glycerol concentration (1 mol L^{-1}) were used, apart from a different alkali (KOH). According to Angelucci et al.,[28] for Au/C materials, replacement of NaOH by KOH does not significantly change the glycerol-electrooxidation performance. Nevertheless, Etesami and Mohamed[41] evidenced that the electrolyte concentration does affect it, notably the glycerol-electrooxidation current density, which increases in the alkali concentration range of 0.1–1 mol L^{-1}. Finally, the effect of the glycerol concentration is more contradictory. On the one hand, a higher glycerol concentration is deleterious due to poisoning of the catalyst surface.[42] On the other hand, it may allow higher current densities to be reached due to the greater availability of fuel.[21] In summary, the combination of all these effects seems to lead to the different shape of the CVs obtained in this study compared to the abovementioned references.

To facilitate the understanding of these results, the FT extended X-ray absorption fine structure (EXAFS) spectra of Au/C and AuAg/C in an alkaline solution in the presence of glycerol at different potentials, reported by Garcia et al.,[32] are shown in Figure 3. Before discussing the spectra, it is of interest to note the electrooxidation mechanism of glycerol on gold in alkaline medium. Gomes et al.[43] proposed a mechanism consisting of the following steps, in which the subscript "ads" represents adsorbed species [Eqs. (1)–(4)]:

$$C_3H_8O_3 + Au - H_2O \rightarrow Au - (C_3H_8O_3)_{ads} + H_2O \quad (1)$$

$$Au - H_2O \rightarrow Au - OH_{ads} + H^+ + e^- \quad (2)$$

$$C - H_2O \rightarrow C - OH_{ads} + H^+ + e^- \quad (3)$$

$$Au - (C_3H_8O_3)_{ads} + Au - OH_{ads} + C - OH \rightarrow Au + C + \text{products} + n\,e^- \quad (4)$$

They also pointed out that oxidized species can be formed from the OH^- present in solution [Eq. (5)]:

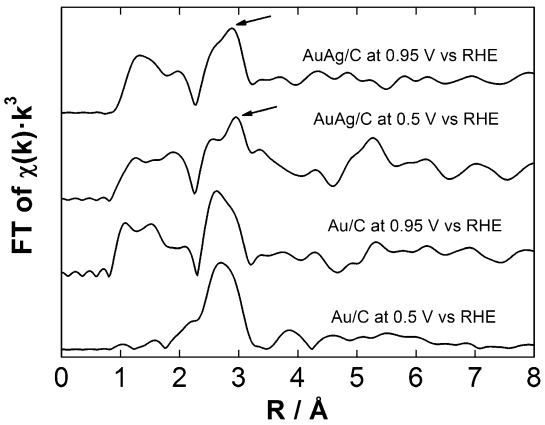

Figure 3. FT EXAFS spectra of Au/C and AuAg/C in 1 mol L^{-1} KOH and 1 mol L^{-1} glycerol at different potentials.

$$Au + OH^- \rightarrow Au - OH + e^- \quad (5)$$

The FT EXAFS spectrum of Au/C shows a peak in the range of 2.3–3 Å associated with the Au–Au distance regardless of the applied potential, and gold-oxide peaks between 1 and 2 Å emerge at the highest potential. In the spectrum of AuAg/C, a first peculiarity is the hump in the signal at about 2.9 Å According to Hannemann et al.,[44] this can be attributed to the formation of an AuAg alloy, in agreement with the results presented by Gomes et al.[34] More interestingly, the presence of Ag induces the appearance of gold-oxide peaks in the FT EXAFS spectra even at low potentials (0.5 V vs. RHE), whereas in the case of the Au/C, the gold-oxide peaks are not present. These oxidized species, which are necessary for glycerol electrooxidation, allow activation of the catalytic gold surface at low potentials in the presence of Ag. Such evidence explains the lower onset potential observed for glycerol electrooxidation. Finally, the differences between these results and those presented in ref. [32] can be explained in terms of the different medium in which the analyses were carried out, which had higher electrolyte (1 mol L^{-1} KOH) and glycerol (1 mol L^{-1}) concentrations.

Interesting information can also be inferred from the nature of the maximum (relative or absolute) current density. Its origin lies in surface poisoning by intermediate reaction products formed during the complex process of glycerol electrooxidation and the formation of some gold oxide at high potentials.[17,20,45,46] All of the bimetallic materials show a relative maximum, with a further increase at higher potentials, in contrast to Au/C. This can be attributed to the electronic effect of Ag on Au, which partially empties the Au 5d band and thus lowers the adsorption strength of the formed adsorbates.[32] Thus, the adsorbed intermediates can more easily undergo desorption, which refreshes the gold surface and thus contributes to the observed second increase in the current density. Finally, Au/C shows the smallest i_f/i_b ratio of the bimetallic materials, indicative of a more pronounced poisoning effect of the intermediates generated in the process of glycerol electrooxidation. The bimetallic materials, in contrast, show higher i_f/i_b ratios reflecting less accumulation of adsorbates on the surface of the

catalyst, especially the Au_3Ag/C catalyst. The significant difference between Au/C and this bimetallic catalysts is further evidence of the beneficial effect of silver on the electrocatalytic activity of gold for glycerol electrooxidation. AuAg/C has an i_f/i_b ratio close to unity and a backward maximum current higher than that of Au_3Ag/C. This suggests a reversible active catalyst surface, in which silver assists in weakening the adsorption strength of the adsorbates and in activating the catalytic surface at lower potential, and makes AuAg/C a promising bimetallic material.

The chronoamperometric curves (Figure 4) confirm the highest electrochemical activity for glycerol oxidation of the AuAg/C material, with the largest mass-normalized current density.

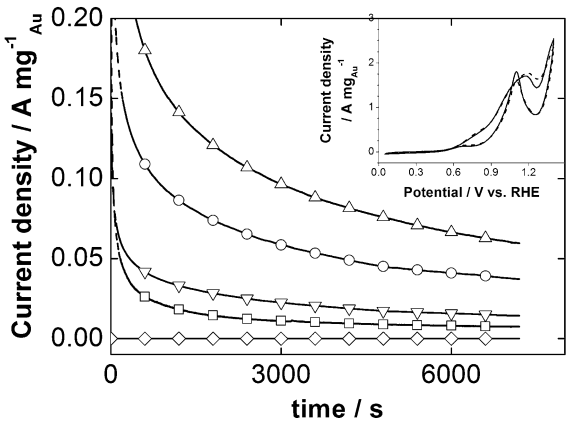

Figure 4. Chronoamperometric curves for the different catalysts at 25 °C in 1 mol L^{-1} KOH and 1 mol L^{-1} glycerol for 2 h. (□: Au/C; ○: Au_3Ag/C; △: AuAg/C; ▽: $AuAg_3/C$; ◇: Ag/C). Inset: CV profiles in 1 mol L^{-1} KOH and 1 mol L^{-1} glycerol before and after chronoamperometry on AuAg/C electrocatalyst.

Au_3Ag/C also shows an enhanced performance compared to Au/C. The less active $AuAg_3/C$ also outperforms Au/C, and this demonstrates the ability of Ag to activate Au as an electrocatalyst. A final interesting feature, shown in the inset of Figure 5, is the almost identical glycerol-electrooxidation CV profile of the AuAg/C catalyst. Although electrolysis for 2 h is not long enough to make solid conclusions about stability, this result preliminarily indicates that the AuAg/C is a stable material, the surface of which remained unaltered after polarization for 2 h.

The activities of the best bimetallic electrocatalyst (AuAg/C) and monometallic Au/C were finally assessed in a single cell. Figure 5 shows the corresponding polarization curves at different temperatures. As representative parameters of the polarization curves, Table 2 lists the open-circuit voltages (OCV) and the maximum power densities (MPD). AuAg/C has higher OCV values than Au/C, which further corroborates the aforementioned activation of gold at lower anodic potentials in the presence of Ag. In terms of the MPD, which is illustrative of the actual fuel-cell performance, both materials show rather similar values, with a slightly higher performance of Au/C, regardless of the operating temperature. However, considering that Au is indeed the active metal in the catalysts, and that the total Au loadings of the two electrodes are different, a normalized comparison in terms of the total gold loading can proposed. Thus, Figure 6 shows the mass-normalized polarization curves at each temperature, calculated by using Equation (6):

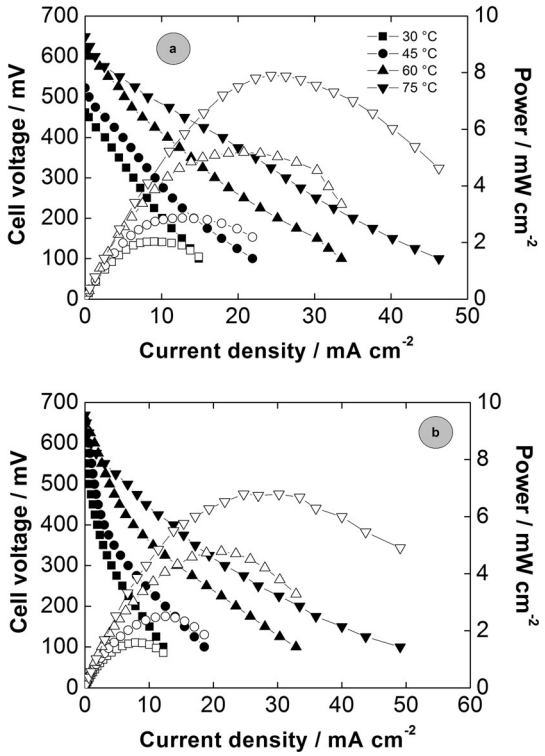

Figure 5. Polarization curves at different temperatures of the catalysts in the single fuel cell. a) Au/C and b) AuAg/C with no backpressure (4 mol L^{-1} KOH and 1 mol L^{-1} glycerol at 1 mL min^{-1} and an oxygen flow of 0.1 L min^{-1}). Metal loading in the anode was 2 mg cm^{-2}, and platinum loading in the cathode was 1 mg cm^{-2}.

Table 2. OCV and MPD of the Au/C and AuAg/C anode catalysts in single-cell measurements.

T [°C]	OCV [mV]		MPD [mW cm^{-2}]	
	Au/C	AuAg/C	Au/C	AuAg/C
30	462	610	2.0	1.6
45	522	625	2.9	2.5
60	612	646	5.2	4.8
75	649	669	7.9	6.8

$$\text{Mass-normalized current} = \frac{j}{m_{Au} \cdot \left(j_{max}/m_{Au,max}\right)} \quad (6)$$

where j is the measured current density for each material [mA cm^{-2}], m_{Au} the corresponding gold loading [mg_{Au} cm^{-2}], j_{max} [mA cm^{-2}] the maximum current density among the two catalysts, and $m_{Au,max}$ the gold loading of the catalyst that shows j_{max}. The mass-normalized polarization curves allow us to verify more clearly the enhancement in the electrochemical performance associated with the presence of Ag in the catalyst

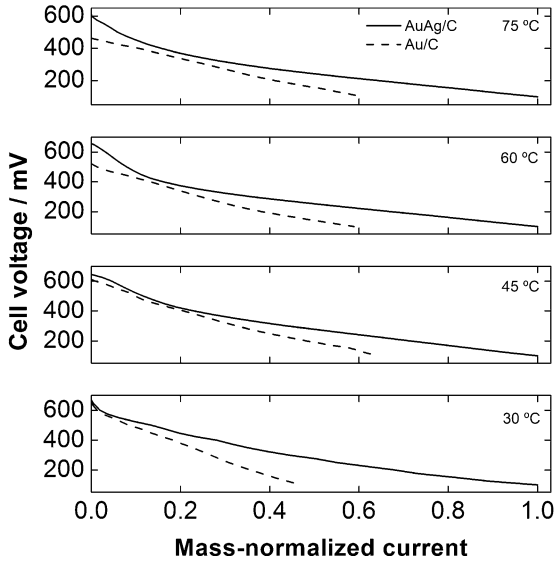

Figure 6. Mass-normalized polarization curves for comparison of Au/C and AuAg/C in terms of mass of gold.

formulation over the entire range of the polarization curves and irrespective of the temperature. The consistency in the performance improvement, even at high current density, is an interesting result. The reaction rate at such values attains its maximum, and it may be expected that the pristine Au/C catalyst would outperform the Au-impoverished AuAg/C catalytic surface. However, the abovementioned positive effects of Ag on Au are expected to facilitate the removal of the products of glycerol electrooxidation, and this makes the Au surface much more active in terms of current density. Finally, product identification in the single cell remains a challenge, and the results of ongoing research thereon will be presented in future works.

3. Conclusions

This study has shown the promoting effect of Ag on the activity of Au in the electrooxidation of glycerol. Cyclic voltammetry showed that silver reduces the onset potential for glycerol electrooxidation and favors renewal of the Au surface by removal of the adsorbed residues, due to the presence of oxidized species at lower potential and the electronic effect of Ag on Au (weakening of the adsorption strength), in spite of the observed electrochemical inactivity of Ag. Chronoamperometric curves confirmed the beneficial effect of the presence of Ag in the catalyst formulation. In particular, bimetallic AuAg/C appears to be the most efficient catalyst, with the lowest onset potential observed by cyclic voltammetry and the highest chronoamperometric current density. This composition seems to have the necessary amount of silver to maximize both promoting effects: the presence of gold oxide, which is mandatory for initiating glycerol electrooxidation at lower potentials, and the decreased adsorption strength of the adsorbates formed during glycerol electrooxidation. Finally, the single-cell results further support the beneficial effect of Ag on Au.

Experimental Section

The synthesis of the AuAg-based catalysts consisted of sonicating 40 mg of XC-72 Vulcan carbon in 50 mL of ultrapure water for 30 min, and then adding a fixed amount of $AuCl_3$ and/or $AgNO_3$ with stirring to promote homogenization. Afterwards, another aqueous solution containing glycerol and NaOH was added to the initial mixture to yield the final concentrations listed in Table 3. The

Table 3. Final concentration of the metal precursors, NaOH, and glycerol used in the synthesis of the carbon-supported catalysts, as well as average particle sizes d_{av} of the materials from TEM images.

Material	$[Au^{3+}]$ [mmol L^{-1}]	$[Ag^{+}]$ [mmol L^{-1}]	[NaOH] [mol L^{-1}]	[Glycerol] [mol L^{-1}]	d_{av} [nm][a]
Au/C	0.4	0			7.3
Au_3Ag/C	0.3	0.1			4.7
AuAg/C	0.2	0.2	0.01	1	4.7
$AuAg_3$/C	0.1	0.3			5.5
Ag/C	0	0.4			34

[a] Values were taken from ref. [33]

black suspensions were kept for 24 h with stirring at room temperature and then washed, filtered, and dried at 80 °C for 12 h. To produce Au/C and Ag/C monometallic catalysts, the method employed was similar, although for these materials the concentrations were 0.40 mmol L^{-1} Au^{3+} and 0.40 mmol L^{-1} Ag^{+}, respectively. The final metal loading of all the materials was approximately 10 %. Information on the main structural parameters of the materials can be found elsewhere.[32–35] As reference parameters, the average particle sizes of the materials from the TEM images in ref. [33] are also listed in Table 3.

To assess the electrocatalytic activity of the materials towards glycerol electrooxidation in alkaline medium, cyclic voltammetry and chronoamperometry (CA) were carried out in a three-electrode glass cell. A nanoparticle-covered glassy carbon electrode (0.385 cm^2, inserted into a Teflon rod), a platinized platinum mesh, and Hg/HgO/KOH (1 mol L^{-1}) were used as working, counter, and reference electrodes, respectively. For the preparation of the working electrode, 1 mg of catalyst was dispersed in 1 mL of isopropyl alcohol. No polymer binder was added, to avoid any interference in the electrochemical response that might hide the actual catalytic performance. With the aid of a chromatographic syringe, the appropriate amount of this suspension was deposited on the glassy carbon support until an approximate metal loading of 100 μg cm^{-2} was achieved. All the potentials are relative to RHE.

The CV sequence consisted of an initial purge with argon for 15 min to remove any traces of oxygen in the working solution, after which a first blank CV in 1 mol L^{-1} KOH as base electrolyte was performed between 0.05 and 1.4 V (vs. RHE). Afterwards, the electrode was immersed in 1 mol L^{-1} KOH and 1 mol L^{-1} glycerol solution and cycled between the same potential limits. The scan rate for these experiments was 10 mV s^{-1}. Measurements were repeated until a stable voltammogram was obtained. CA was carried out at a fixed potential of 0.726 V versus RHE for 2 h in the same reaction medium as for CV. This potential was high enough to reach substantial conclusions on the activity of all the materials for the electrooxidation of glycerol without being an excessively high anodic potential (unfavorable from a practical point of view). FT of

the EXAFS analysis of the Au/C and AuAg/C catalysts was performed on X-ray absorption spectra (XAS) presented by Garcia et al.[32] with the aid of the WINXAS 3.0 software.

For the best bimetallic material and the reference Au/C, fuel cell electrodes were prepared as follows: a thick ink consisting of Au/C or the bimetallic material, Nafion emulsion (10 wt% with respect to the carbon loading in the catalytic layer, binder for the catalytic layer), and isopropyl alcohol as solvent was prepared and deposited by paint brush onto a catalytic layer[21] until a metal loading of 2 mg cm^{-2} was reached The cathode was prepared with commercial BASF Fuel Cells 20% Pt/C by the same procedure. The Pt loading was 1 mg cm^{-2}. The MEA was prepared by sandwiching a piece of PBI (Danish Power System, Daposy, Denmark) between the electrodes membrane. To provide anionic conductivity, the membrane was immersed in 4 mol L^{-1} KOH for at least one week. The electrochemical measurements were carried out with the aid of a potentiostat/galvanostat (AUTOLAB PGSTAT 302; Metrohm Autolab B.V., The Netherlands) in potentiostatic mode, from OCV to lower cell voltages. The anode was fed with 1 mol L^{-1} glycerol and 4 mol L^{-1} KOH at a flow rate of 1 mL min^{-1}, whereas in the cathode oxygen was fed at a flow rate of 30 sccm. The active area of the electrode was 4 cm^2. The cell hardware is described elsewhere.[21]

Acknowledgements

The authors thank Fundação de Amparo a Pesquisa do Estado de São Paulo (FAPESP) process number 2012/10856-7 for financial support, and 2012/05627-9 for the postdoctoral fellowship and scholarship for the undergraduate student E.B.F., and are grateful to the Conselho Nacional de Desenvolvimento Científico e Tecnológico (CNPq) for the scholarship awarded to the undergraduate student J. C. (Progama de Iniciação Científica).

Keywords: electrochemistry · fuel cells · gold · oxidation · silver

[1] Renewable Energy Policy Network for the 21st century, Renewable 2014: Status Report. http://www.ren21.net/Portals/0/documents/Resources/GSR/2014/GSR2014_full%20report_low%20res.pdf (accessed January 2015).
[2] http://www.iea.org/topics/biofuels/ (accessed January 2015).
[3] P. F. F. Amaral, T. F. Ferreira, G. C. Fontes, M. A. Z. Coelho, *Food Bioprod. Process.* **2009**, *87*, 179 – 186.
[4] Y.-C. Lin, *Int. J. Hydrogen Energy* **2013**, *38*, 2678 – 2700.
[5] C. Varrone, R. Liberatore, T. Crescenzi, G. Izzo, A. Wang, *Appl. Energy* **2013**, *105*, 349 – 357.
[6] S. Abad, X. Turon, *Biotechnol. Adv.* **2012**, *30*, 733 – 741.
[7] R. A. Sheldon, *Green Chem.* **2014**, *16*, 950 – 963.
[8] J. C. Beltrán-Prieto, K. Kolomazník, J. Pecha, *Aust. J. Chem.* **2013**, *66*, 511 – 521.
[9] K. Matsuoka, Y. Iriyama, T. Abe, M. Matsuoka, Z. Ogumi, *J. Power Sources* **2005**, *150*, 27 – 31.
[10] S. R. Ragsdale, C. B. Ashfield, *ECS Trans.* **2008**, *16*, 1847 – 1854.
[11] R. L. Arechederra, S. D. Minteer, *Fuel Cells* **2009**, *9*, 63 – 69.
[12] V. Bambagioni, C. Bianchini, A. Marchionni, J. Filippi, F. Vizza, J. Teddy, P. Serp, M. Zhiani, *J. Power Sources* **2009**, *190*, 241 – 251.
[13] A. Ilie, M. Simoes, S. Baranton, C. Coutanceau, S. Martemianov, *J. Power Sources* **2011**, *196*, 4965 – 4971.
[14] G. Rotko, S. S. Kurek, *Chemik* **2011**, *65*, 1011 – 1018.
[15] Z. Zhang, L. Xin, Z. Wang, W. Li, *Cogeneration of electricity and valuable chemicals: Electrocatalytic oxidation of glycerol in anion-exchange membrane fuel cell*, in AIChE 2012 – 2012 AIChE Annual Meeting, Conference Proceedings, **2012**.
[16] Z. Zhang, L. Xin, W. Li, *Appl. Catal. B* **2012**, *119 – 120*, 40 – 48.
[17] Z. Zhang, L. Xin, W. Li, *Int. J. Hydrogen Energy* **2012**, *37*, 9393 – 9401.
[18] J. Qi, L. Xin, Z. Zhang, K. Sun, H. He, F. Wang, D. Chadderdon, Y. Qiu, C. Liang, W. Li, *Green Chem.* **2013**, *15*, 1133 – 1137.
[19] S. Yongprapat, A. Therdthianwong, S. Therdthianwong, *J. Appl. Electrochem.* **2012**, *42*, 483 – 490.
[20] S. Yongprapat, S. Therdthianwong, A. Therdthianwong, *Electrochim. Acta* **2012**, *83*, 87 – 93.
[21] A. P. Nascimento, J. J. Linares, *J. Braz. Chem. Soc.* **2014**, *25*, 509 – 516.
[22] S. Authayanun, M. Mamlouk, K. Scott, A. Arpornwichanop, *Appl. Energy* **2013**, *109*, 192 – 201.
[23] L. Xin, Z. Zhang, W. Li, *Simultaneous generation of mesoxalic acid and electricity from glycerol on Au anode catalyst in anion exchange membrane fuel cell reactors,* in AIChE 2012 – 2012 AIChE Annual Meeting, Conference Proceedings, **2012**.
[24] Z. Zhang, L. Xin, J. Qi, Z. Wang, W. Li, *Green Chem.* **2012**, *14*, 2150 – 2152.
[25] L. Xin, Z. Zhang, Z. Wang, W. Li, *ChemCatChem* **2012**, *4*, 1105 – 1114.
[26] Z. Zhang, L. Xin, J. Qi, D. J. Chadderdon, K. Sun, K. M. Warsko, W. Li, *Appl. Catal. B* **2014**, *147*, 871 – 878.
[27] D. Padayachee, V. Golovko, A. T. Marshall, *Electrochim. Acta* **2013**, *98*, 208 – 217.
[28] C. A. Angelucci, H. Varela, G. Tremiliosi-Filho, J. F. Gomes, *Electrochem. Commun.* **2013**, *33*, 10 – 13.
[29] F. Colmati, E. Antolini, E. R. Gonzalez, *J. Power Sources* **2006**, *157*, 98 – 103.
[30] C. Jin, Z. Zhang, Z. Chen, Q. Chen, *Int. J. Electrochem. Sci.* **2013**, *8*, 4215 – 4224.
[31] Y. Kim, H. Kim, W. B. Kim, *Electrochem. Commun.* **2014**, *46*, 36 – 39.
[32] A. G. Garcia, P. P. Lopes, J. F. Gomes, C. Pires, E. B. Ferreira, R. G. M. Lucena, L. H. S. Gasparotto, G. Tremiliosi-Filho, *New J. Chem.* **2014**, *38*, 2865 – 2873.
[33] J. F. Gomes, A. C. Garcia, L. H. S. Gasparotto, N. E. de Souza, E. B. Ferreira, C. Pires, G. Tremiliosi-Filho, *Electrochim. Acta* **2014**, *144*, 361 – 368.
[34] J. F. Gomes, A. C. Garcia, C. Pires, E. B. Ferreira, R. Q. Albuquerque, G. Tremiliosi-Filho, L. H. S. Gasparotto, *J. Phys. Chem. C* **2014**, *118*, 28868 – 28875.
[35] E. B. Ferreira, J. F. Gomes, G. Tremiliosi-Filho, L. H. S. Gasparotto, *Mater. Res. Bull.* **2014**, *55*, 131 – 136.
[36] A. E. S. Sleightholme, J. R. Varcoe, A. R. Kucernak, *Electrochem. Commun.* **2008**, *10*, 151 – 155.
[37] S. S. Abd El Rehim, H. H. Hassan, M. A. M. Ibrahim, M. A. Amin, *Monatsh. Chem.* **1998**, *129*, 1103 – 1117.
[38] A. T. Marshall, V. Golovko, D. Padayachee, *Electrochim. Acta* **2015**, *153*, 370 – 378.
[39] J. L. Bott-Neto, A. C. Garcia, V. L. Oliveira, N. E. De Souza, G. Tremiliosi-Filho, *J. Electroanal. Chem.* **2014**, *735*, 57 – 62.
[40] V. V. Sobyanin, N. Gorodetskii, N. Bulgakov, *React. Kinet. Catal. Lett.* **1977**, *7*, 285 – 290.
[41] M. Etesami, N. Mohamed, *Int. J. Electrochem. Sci.* **2011**, *6*, 4676 – 4689.
[42] J. F. Gomes, C. A. Martins, M. J. Giz, G. Tremiliosi-Filho, G. A. Camara, *J. Catal.* **2013**, *301*, 154 – 161.
[43] J. F. Gomes, L. H. S. Gasparotto, G. Tremiliosi-Filho, *Phys. Chem. Chem. Phys.* **2013**, *15*, 10339 – 10349.
[44] S. Hannemann, J.-D. Grunwaldt, F. Krumeich, P. Kappen, A. Baiker, *Appl. Surf. Sci.* **2006**, *252*, 7862 – 7873.
[45] A. N. Geraldes, D. F. Silva, J. C. M. Silva, R. F. B. Souza, E. V. Spinacé, A. O. Neto, M. Linardi, M. C. Santos, *J. Braz. Chem. Soc.* **2014**, *25*, 831 – 840.
[46] J. H. Song, J. Y. Yu, M. Z. Zhang, Y. J. Liang, C. W. Xu, *Int. J. Electrochem. Sci.* **2012**, *7*, 4362 – 4368.

Received: January 22, 2015
Published online on April 20, 2015